Line of Sight Angular Rate Estimation Based on Robust Cubature Kalman Filter with Standard Trajectory Uncertainties

Xitong Sun, Xingbai Luo, Min Gao, Xiaodong Zhou, Shiyue Zhang

Abstract—**Aiming at the problem that inertial measurement element is not suitable for low-cost guided ammunition, a method for estimating the line of sight (LOS) angular rate of missile motion parameters instead of inertial measurement element is designed. Based on the missile target motion model and seeker measurement model, a LOS angular rate filtering model is constructed. Aiming at the characteristics of nonlinearity and parameter uncertainty of the model, robust cubature Kalman filter (RCKF) is proposed to transform the filtering problem of the uncertain filtering model into the problem of minimizing the upper bound with parameter error covariance. Compared with the cubature Kalman filter (CKF), the effectiveness and robustness of RCKF were verified by digital simulation. The experimental results showed that RCKF was effective and its accuracy was slightly better than CKF under the condition of small disturbance; Under the condition of large disturbance, the maximum error of LOS inclination angle decreased by 55.56%, the standard deviation decreased by 55.53%. The maximum error of LOS deflection angle decreased by 56.5%, the standard deviation decreased by 55.51%. The maximum error of LOS inclination angle rate decreased by 53.92%. The standard deviation decreased by 55.96%. The maximum error of LOS deflection angle rate decreased by 55.57%, the standard deviation decreased by 55.41%.**

Index Terms—**LOS angular rate; Kalman filter; robustness; parameter uncertainty**

I. Introduction

The strapdown seeker has the characteristics of small volume, light weight and high reliability. It is widely used in modern guided weapons[1]. But the strapdown seeker is fixed with the missile body, and the line of sight (LOS) angle and altitude angle of missile target are coupled with each other, so the seeker can not directly give the LOS angle and LOS angular rate required for guidance. The LOS angular rate of missile and target needs to be solved by constructing appropriate decoupling model and estimation algorithm.

Scholars at home and abroad had carried out extensive and in-depth researches on the estimation of LOS angular rate of all strapdown missiles. With the development of microprocessors, from the initial jitter adaptive filtering and differential network, it has been developed to use nonlinear Kalman filter to estimate LOS rate. In reference [2], firstly, altitude angle and angular velocity are estimated by unscented Kalman filter, and then LOS angle and LOS angular rate were estimated by tracking differentiator. The estimation error of LOS angular rate was less than 0.06 o/s. In reference [3], the extended model of state equation was established, and the fifth-order CKF suitable for high-dimensional model was used to effectively improve the filtering accuracy of LOS angular rate. In reference [4], the influence of altitude error on the LOS rate after filtering was considered, and it was concluded that the altitude angle came from inertial measurement element rather than filtering, which was more conducive to improving the accuracy of LOS angular rate. In reference [5], the second-order and third-order fixed gain filters were used to estimate the LOS rate and the maneuverability of the target. In reference [6], a finite time LOS rate estimation was proposed. Through geometric uniformity and Lyapunov theory, it was proved that the estimation error can converge to zero in finite time. In reference [7], tracking filter was used to reduce missile attitude measurement noise, and cubature Kalman filter was used to improve LOS rate estimation accuracy. At present, the uncertainty of model, measurement system and noise are ignored in Kalman filtering of LOS angular rate. The model and measurement system are considered to be accurate, the noise is standard Gaussian noise, and the influence of model uncertainty on filtering performance is not considered[8].

The uncertainty of the system will lead to inaccurate filtering results and even divergence. LOS angular rate estimation needs a filtering method which can guarantee the filtering accuracy and robustness under the system uncertainty. With the development of Kalman filter, scholars have given a variety of robust Kalman filtering algorithms, whose basic principle is to control the filter gain to ensure the robustness of the filter[9]. Common methods include $H\infty$ filter[10], adjusting factor method[11], intelligent control[12], unknown input observer[13], etc. $H\infty$ filter lowers the computational efficiency, intelligent control can not guarantee the stability of the closed-loop system, and the unknown input observer is powerless for complex nonlinear systems[14]. Therefore, this paper selects the adjustment factor method to construct the

Manuscript received Nov 02, 2020; revised February 26, 2021.

Xitong Sun is a doctoral student in Ammunition Engineering Department, Army Engineering University, No. 97 Heping West Road, Shijiazhuang, Hebei, 050003, China. (e-mail: 417006576@qq.com)

Xingbai Luo is a professor in Ammunition Engineering Department, Army Engineering University, No. 97 Heping West Road, Shijiazhuang, Hebei, 050003, China. (e-mail: gli210035@gmail.com)

Min Gao is a professor in Missile Engineering Department, Army Engineering University, No.97 Heping West Road, Shijiazhuang, Hebei, 050003, China.(e-mail: gaomin1100@163.com)

Xiaodong Zhou a professor is in Ammunition Engineering Department, Army Engineering University, No. 97 Heping West Road, Shijiazhuang, Hebei, 050003, China. (corresponding author, phone: 18515661302, e-mail: zhouxiaodong202010@163.com)

Shiyue Zhang is an assistant in Army Engineering University, No. 97 Heping West Road, Shijiazhuang, Hebei, 050003, China. (e-mail: sxqty2020@163.com)

LOS rate filtering estimation algorithm with uncertainty, and the adjustment factor is obtained by the lemma in this paper.

All the above filtering methods need inertial measurement unit (IMU) to measure the angular rate of missile body. The application of inertial measurement unit will bring about a substantial increase in cost, and has the problems of low anti overload ability and accuracy affected by the environment. In order to reduce the cost of guided ammunition, a robust cubature Kalman filter (RCKF) LOS angular rate estimation algorithm based on the reference trajectory is proposed for its trajectory with small disturbance motion around the reference trajectory and attacking the fixed target. It is based on the relative motion model of missile and target and the measurement model of seeker. The trajectory parameters are regarded as uncertain model parameters.

II. Common Coordinate System and Angle Definition

(1) $O-x_b y_b z_b$ is the ground coordinate system. The origin O of the coordinate system is set on the instantaneous mass center of the projectile. The Ox_b axis points to the firing direction along the horizontal line. The Oy_b axis is straight up. Oz_b is perpendicular to the other two axes and forms a right-handed coordinate system.

(2) $O-x_2 y_2 z_2$ is the ballistic coordinate system. The coordinate origin O is set on the instantaneous mass center of the missile body. The Ox_2 axis coincides with the velocity vector of ammunition. Oy_2 is located in the vertical plane containing the velocity vector and perpendicular to the Ox_2 axis. The Oz_2 axis is perpendicular to the other two axes and forms a right-handed coordinate system.

(3) $O-x_q y_q z_q$ is the LOS coordinate system. The origin O of the coordinate system is set on the instantaneous mass center of the missile body. The Ox_q axis and the missile-target connecting line coincide and point to the target. The Oz_q axis lies in the $Ox_b z_b$ plane of the datum system and it is perpendicular to the Ox_q axis. The Oy_q axis is perpendicular to the other two axes and forms a right-handed coordinate system.

(4) $O-x_1 y_1 z_1$ is the missile body coordinate system. The origin O of the coordinate system is set on the instantaneous mass center of the missile body. The Ox_1 axis coincides with the longitudinal axis of the missile body and points to the head positively. The Oy_1 axis is located in the longitudinal symmetry plane of the missile body and perpendicular to the Ox_1 axis. Oz_1 is perpendicular to the plane $Ox_1 y_1$, and its direction is determined by the right-hand rectangular coordinate system.

(5) $O-x_l y_l z_l$ is the body line of sight (BLOS) coordinate system. The origin O of the coordinate system is set on the instantaneous mass center of the missile body. The Ox_l axis coincides with the LOS of the missile and the target and points to the target. The Oz_l axis is located in the $Ox_1 z_1$ plane of the missile body coordinate system and is perpendicular to the Ox_l axis. Oy_l is perpendicular to the other two axes and forms a right-handed coordinate system.

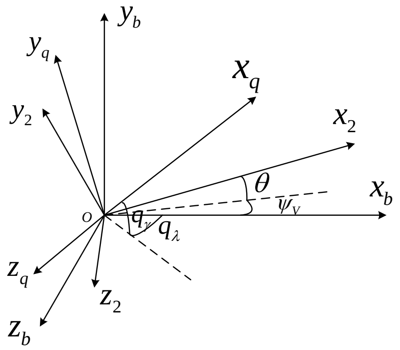

(a) Definitions of the reference coordinate, ballistic coordinate and LOS coordinate

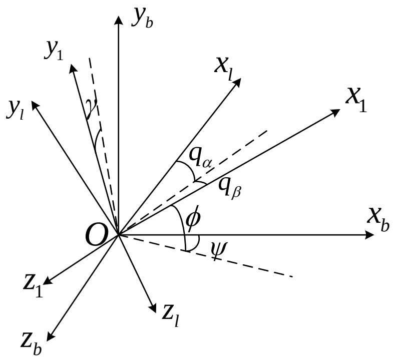

(b) Definitions of the body coordinate and BLOS coordinate

Fig. 1. Definition of coordinate

TABLE I
DEFINITION OF BASIC ANGLE

Symbol	Name	Definition
ϕ	Pitch angle	Angle between Ox_1 axis and horizontal plane
ψ	Yaw angle	Angle between projection of longitudinal axis of projectile in horizontal plane and axis Ox_b
γ	Roll angle	Angle between Oy_1 axis and plumb plane containing longitudinal axis of projectile
θ	Trajectory inclination	Angle between Ox_2 axis and horizontal plane
ψ_V	Ballistic deflection angle	Angle between the projection of axis Ox_2 in horizontal plane and axis Ox_b
q_γ	Line of sight inclination	Angle between axis Ox_q and horizontal plane
q_λ	Line of sight deviation	Angle between the projection of axis Ox_q in horizontal plane and axis Ox_b
q_α	Body line of sight inclination	Angle between axis Ox_l and plane $Ox_1 z_1$ of projectile system
q_β	Body line of sight deflection angle	Angle between projection of axis Ox_l in plane $Ox_1 z_1$ of projectile system and Ox_l
q_c	Line of sight transformation angle	Angle between axis Oy_q and axis Oy_l

The transformation matrix between coordinate systems is shown in Fig. 2. The transformation matrix between each coordinate system is represented by $L()$.

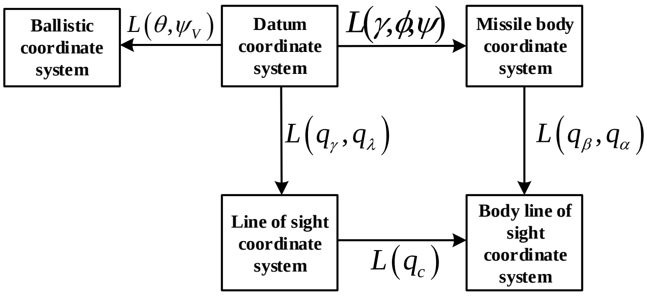

Fig. 2. Relationships of coordinate systems

III. Modeling of Projectile Motion Model

A. Dynamic equation of projectile centroid motion

The dynamic equation of projectile centroid motion is established in the ballistic coordinate system, as shown below[15][16]:

$$\begin{cases} m\dfrac{dv}{dt} = G_{x_2} + R_{x_2} \\ mv\dfrac{d\theta}{dt} = G_{y_2} + R_{y_2} \\ -mv\cos\theta\dfrac{d\psi_v}{dt} = G_{z_2} + R_{z_2} \end{cases} \tag{1}$$

Where, m ——refers to projectile mass;

v ——refers to projectile velocity;

t ——refers to time;

θ ——refers to trajectory inclination angle;

ψ_v ——refers to ballistic deflection angle;

$G_{x_2}, G_{y_2}, G_{z_2}$ ——refer to the components of gravity in the ballistic coordinate system respectively;

$R_{x_2}, R_{y_2}, R_{z_2}$ ——refer to the components of aerodynamic force in the ballistic coordinate system respectively.

B. Dynamic equation of projectile rotating around the center of mass

The kinetic equation of projectile rotating around the center of mass is established in the quasi projectile coordinate system, as shown below[15][16]:

$$\begin{bmatrix} J_{x_4}\dfrac{d\omega_{x_4}}{dt} \\ J_{y_4}\dfrac{d\omega_{y_4}}{dt} \\ J_{z_4}\dfrac{d\omega_{z_4}}{dt} \end{bmatrix} = \begin{bmatrix} M_{x_4} \\ M_{y_4} \\ M_{z_4} \end{bmatrix} - \begin{bmatrix} 0 \\ (J_{x_4} - J_{z_4})\omega_{x_4}\omega_{z_4} \\ (J_{y_4} - J_{x_4})\omega_{x_4}\omega_{y_4} \end{bmatrix} \tag{2}$$

Where, $J_{x_4}, J_{y_4}, J_{z_4}$ ——refer to the moment of inertia of the projectile to each axis of the quasi projectile coordinate system respectively;

$\omega_{x_4}, \omega_{y_4}, \omega_{z_4}$ —— refer to the components of rotational angular velocity ω on each axis of quasi projectile coordinate system respectively;

$M_{x_4}, M_{y_4}, M_{z_4}$ —— refer to the components of aerodynamic moment in the quasi projectile coordinate system respectively.

C. Kinematic equation of projectile centroid motion

$$\begin{cases} \dfrac{dx}{dt} = v\cos\theta\cos\psi_V \\ \dfrac{dy}{dt} = v\sin\theta \\ \dfrac{dz}{dt} = -v\cos\theta\sin\psi_V \end{cases} \tag{3}$$

Where x, y, z ——refer to three axis coordinates of projectile in the inertial system respectively[15][16].

D. Kinematic equation of projectile rotating around the center of mass

$$\begin{cases} \dfrac{d\phi}{dt} = \omega_{z_4} \\ \dfrac{d\psi}{dt} = \dfrac{1}{\cos\phi}\omega_{y_4} \\ \dfrac{d\gamma}{dt} = \omega_{x_4} - \omega_{y_4}\tan\phi \end{cases} \tag{4}$$

Where, ϕ ——refers to pitch angle;

ψ ——refers to yaw angle;

γ ——refers to roll angle[15][16][17].

E. Geometric relation equation

$$\begin{cases} \beta = \arcsin\left[\cos\theta\sin(\psi - \psi_v)\right] \\ \alpha = \phi - \arcsin\left(\dfrac{\sin\theta}{\cos\beta}\right) \\ \gamma_v = \arcsin(\tan\theta\tan\beta) \end{cases} \tag{5}$$

Where, α ——refers to angle of attack;

β ——refers to sideslip angle;

γ_v ——refers to velocity tilt angle[15][16].

IV. Line of Sight Decoupling Algorithm for Strapdown Seeker

A. Relative motion model of missile and target

The relative motion model of missile and target is established, as shown in Fig. 3. Among them, M is the position of the missile body, T is the position of the target point, $\boldsymbol{v}$ is the velocity of the missile body, $Oxyz$ is the ground coordinate system, v_x, v_y, v_z is the projection of the projectile velocity $\boldsymbol{v}$ on the three coordinate axes of the LOS coordinate system, and the target motion vector is $\boldsymbol{v_t}$.

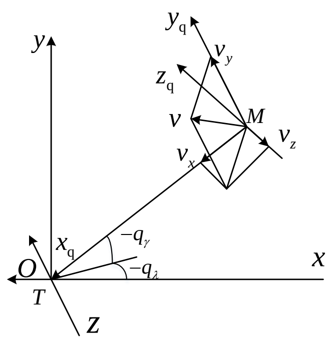

Fig. 3. Relative motion between projectile and target

The change rule of r can be expressed as

$$\dot{\boldsymbol{r}} = \boldsymbol{v} - \boldsymbol{v_t} \tag{6}$$

Since terminal guidance ammunition usually strikes fixed targets, $\boldsymbol{v_t} = 0$.

In order to analyze the change rule of LOS angle, $\boldsymbol{r}$ is expressed in polar coordinates: $\boldsymbol{r} = \begin{pmatrix} r & q_\gamma & q_\lambda \end{pmatrix}$. In the LOS coordinate system, the instantaneous motion of missile body can be decomposed into two circular motions around target point T in Ox_qy_q plane and Ox_qz_q plane with relative distance r as radius. According to the relationship between angular velocity of circular motion and linear velocity, the expression of relative velocity of projectile and target is obtained:

$$\begin{cases} \dot{r} = v_x \\ \dot{q}_\gamma = -\dfrac{v_y}{r} \\ \dot{q}_\lambda = -\dfrac{v_z}{r\cos(q_\gamma)} \end{cases} \tag{7}$$

It is known that the coordinates of projectile velocity in the ballistic coordinate system is $(v, 0, 0)$. Based on the coordinate transformation relations among the ballistic coordinate system, LOS coordinate system and ground coordinate system, the projection of projectile velocity vector in the LOS coordinate system can be obtained:

$$\begin{bmatrix} v_x \\ v_y \\ v_z \end{bmatrix} = L(q_\gamma, q_\lambda) L(\psi_v, \theta) \begin{bmatrix} v \\ 0 \\ 0 \end{bmatrix} \tag{8}$$

The velocity component of missile body in the LOS coordinate system obtained from formula (8) is introduced into equation (7). Finally, the relative motion model of missile and target is obtained:

$$\begin{bmatrix} \dot{r} \\ \dot{q}_\lambda \\ \dot{q}_\gamma \end{bmatrix} = \begin{bmatrix} v(\sin q_\gamma \sin\theta + \cos q_\gamma \cos\theta \cos(q_\lambda - \psi_v)) \\ \dfrac{-v\cos\theta \sin(q_\lambda - \psi_v)}{r\cos q_\gamma} \\ \dfrac{v(\cos\theta \sin q_\gamma \cos(q_\lambda - \psi_v) - \sin\theta \cos q_\gamma)}{r} \end{bmatrix} + \begin{bmatrix} w_1 \\ w_2 \\ w_3 \end{bmatrix} \tag{9}$$

Where w_1, w_2 and w_3 represent state model noise respectively.

B. Measurement model of seeker

The coordinates of the LOS between the ammunition and the target in the ground coordinate system are $|\boldsymbol{r}| \cdot (\cos q_\gamma \cos q_\lambda, \sin q_\gamma, -\cos q_\gamma \sin q_\lambda)$. Its coordinates in the missile body system are a $|\boldsymbol{r}| \cdot (\cos q_\alpha \cos q_\beta, \sin q_\alpha, -\cos q_\alpha \sin q_\beta)$. According to the transformation relationship $L(\psi, \vartheta, \gamma)$ between the missile body coordinate system and ground coordinate system, it can be concluded that:

$$\begin{bmatrix} \cos q_\gamma \cos q_\lambda \\ \sin q_\gamma \\ -\cos q_\gamma \sin q_\lambda \end{bmatrix} = L(\psi, \phi, \gamma) \begin{bmatrix} \cos q_\alpha \cos q_\beta \\ \sin q_\alpha \\ -\cos q_\alpha \sin q_\beta \end{bmatrix} \tag{10}$$

Finally, the measurement model of all strapdown laser seeker is simplified:

$$\begin{bmatrix} q_\alpha \\ q_\beta \end{bmatrix} = \begin{bmatrix} \arcsin(R_{21}\cos q_\gamma \cos q_\lambda + R_{22}\sin q_\gamma - R_{23}\cos q_\gamma \sin q_\lambda) \\ -\arctan\left(\dfrac{R_{31}\cos q_\lambda + R_{32}\tan q_\gamma - R_{33}\sin q_\lambda}{R_{11}\cos q_\lambda + R_{12}\tan q_\gamma - R_{13}\sin q_\lambda}\right) \end{bmatrix} + \begin{bmatrix} v_1 \\ v_2 \end{bmatrix} \tag{11}$$

Where R_{ij} is the element in the transformation matrix from the ground coordinate system to the missile body coordinate system, and v_1 and v_2 are the measurement noise of seeker.

V. Design Robust Cubature Kalman Filter

A. Linearization of filtering model

A discrete nonlinear system with uncertain parameters is established as follows:

$$\begin{cases} \boldsymbol{x}_{k+1} = f(\boldsymbol{x}_k, \boldsymbol{u}_k, \tilde{\boldsymbol{A}}_k) + \boldsymbol{w}_k \\ \boldsymbol{y}_{k+1} = h(\boldsymbol{x}_{k+1}, \tilde{\boldsymbol{B}}_{k+1}) + \boldsymbol{v}_{k+1} \end{cases} \tag{12}$$

Where $\boldsymbol{x}_k \in R^n$ is the state variable matrix of the system and $\boldsymbol{y}_k \in R^m$ is the observation matrix of the system. $\boldsymbol{u}_k$ is the input matrix of the system, $f(\cdot)$ and $h(\cdot)$ are the nonlinear state equation and measurement equation of the system respectively. $\tilde{\boldsymbol{A}}_k \in R^l$ is the parameter matrix of the state model with uncertainty, and $\tilde{\boldsymbol{B}}_k \in R^s$ is the parameter matrix of the measurement model with uncertainty. $\boldsymbol{w}_k \in R^n$ and $\boldsymbol{v}_k \in R^m$ are mutually uncorrelated white Gaussian noise matrices with zero mean values. The covariance at any time satisfies the following conditions:

$$E(\begin{bmatrix} \boldsymbol{w}_k \\ \boldsymbol{v}_{k+1} \end{bmatrix} \begin{bmatrix} \boldsymbol{w}_k & \boldsymbol{v}_{k+1} \end{bmatrix}) = \begin{bmatrix} \boldsymbol{Q}_k & \\ & \boldsymbol{R}_{k+1} \end{bmatrix} \tag{13}$$

The state equation and measurement equation of nonlinear system are expanded at the filter state estimation point by Taylor formula. The linear system is obtained:

$$\begin{cases} \boldsymbol{x}_{k+1} = f(\hat{\boldsymbol{x}}_k, \tilde{\boldsymbol{A}}_k) + \left.\dfrac{\partial f(\boldsymbol{x}_k, \boldsymbol{u}_k, \tilde{\boldsymbol{A}}_k)}{\partial \boldsymbol{x}_k}\right|_{\boldsymbol{x}_k = \hat{\boldsymbol{x}}_k} \bullet \tilde{\boldsymbol{x}}_k \\ +O(\tilde{\boldsymbol{x}}_k{}^2) + \boldsymbol{w}_k \\ \boldsymbol{y}_{k+1} = h(\hat{\boldsymbol{x}}_{k+1}, \tilde{\boldsymbol{B}}_{k+1}) + \left.\dfrac{\partial h(\boldsymbol{x}_{k+1}, \tilde{\boldsymbol{B}}_{k+1})}{\partial \boldsymbol{x}_{k+1}}\right|_{\boldsymbol{x}_{k+1} = \hat{\boldsymbol{x}}_{k+1}} \bullet \tilde{\boldsymbol{x}}_{k+1} \\ +O(\tilde{\boldsymbol{x}}_{k+1}{}^2) + \boldsymbol{v}_{k+1} \end{cases} \tag{14}$$

Where $\hat{\boldsymbol{x}}$ is the estimated value of the system state by the filter, and $\tilde{\boldsymbol{x}}$ is the state estimation error value. $O(\tilde{\boldsymbol{x}}^2)$ is the higher order term in Taylor series.

B. Linearization of the coefficients of the first order term of the filtering model

The first-order coefficients are nonlinear functions. Taylor expansion is carried out with parameters as independent variables:

$$g(\tilde{\boldsymbol{A}}_k) = g(\bar{\boldsymbol{A}}_k) + \left.\frac{\partial g(\tilde{\boldsymbol{A}}_k)}{\partial \tilde{\boldsymbol{A}}_k}\right|_{\tilde{\boldsymbol{A}}_k = \bar{\boldsymbol{A}}_k} \bullet (\Delta \boldsymbol{A}_k) + O(\Delta \boldsymbol{A}_k{}^2) \tag{15}$$

Where, $\bar{A}$ is the determined value of the nonlinear system parameters. ΔA_k is the uncertainty of the parameter. Since the range of ΔA_k is generally very small, the high-order small term $O(\Delta A_k{}^2)$ can be ignored. It is known that the coefficient matrix consists of definite and uncertain terms. In order to facilitate the derivation of the algorithm, the linearized first-order coefficients of the state equation can be expressed as follows:

$$g_1(\tilde{A}_k)=\left.\frac{\partial f(x_k,u_k,\tilde{A}_k)}{\partial x_k}\right|_{x_k=\hat{x}_k}=F_{1,k}+M_{1,k}\Gamma_{1,k}N_{1,k} \tag{16}$$

Where $F_{1,k}$ is the coefficient determinate term of the linearized system at k time, and $M_{1,k}\Gamma_{1,k}N_{1,k}$ is the coefficient uncertainty term. $M_{1,k}$ and $N_{1,k}$ are matrices with corresponding dimensions, expressing accurately the uncertainty boundary of system parameters. $\Gamma_{1,k}$ is an unknown bounded time-varying matrix, that is, $\Gamma_{1,k}{}^{\mathrm{T}}\Gamma_{1,k}\le I$. From formula (15) and (16), the corresponding relationship of two forms can be easily obtained:

$$\begin{cases} F_{1,k}=g_1(\bar{A}_k) \\ M_{1,k}\Gamma_{1,k}N_{1,k}=\partial g_1(\tilde{A}_k)/\partial\tilde{A}_k\big|_{\tilde{A}_k=\bar{A}_k}\bullet(\Delta A_k) \end{cases} \tag{17}$$

It can be concluded from the above formula that the coefficient uncertainty of the first order term of the state equation is completely determined by the parameter uncertainty ΔA_k in the nonlinear system. If the maximum uncertainty of the model parameter is known, it can be set as follows:

$$\begin{cases} M_{1,k}=\partial g_1(\tilde{A}_k)/\partial\tilde{A}_k\big|_{\tilde{A}_k=\bar{A}_k}\bullet\max\left(\mathrm{abs}\left(\Delta A_k\right)\right) \\ N_{1,k}=I_{n\times n} \end{cases} \tag{18}$$

Where abs is the absolute value of each element in the matrix.

Similarly, the first order uncertainty coefficient of the measurement equation can be set as follows:

$$\left.\frac{\partial h(x_{k+1},\tilde{B}_{k+1})}{\partial x_{k+1}}\right|_{x_{k+1}=\hat{x}_{k+1}}=H_{2,k+1}+M_{2,k+1}\Gamma_{2,k+1}N_{2,k+1} \tag{19}$$

The definitions of Γ_2 and N_2 are the same as those of Γ_1 and N_1 above. H_2 and M_2 can be obtained from the maximum uncertainty of measuring model parameters:

$$\begin{cases} H_{2,k+1}=g_2(\tilde{B}_{k+1}) \\ M_{2,k+1}=\partial g_2(\tilde{B}_{k+1})/\partial\tilde{B}_{k+1}\big|_{\tilde{B}_{k+1}=\bar{B}_{k+1}}\bullet\max\left(\mathrm{abs}\left(\Delta B_{k+1}\right)\right) \end{cases} \tag{20}$$

According to formula (14)~(20), the expression of linearized system with uncertain parameters is obtained:

$$\begin{cases} x_{k+1}=f(\hat{x}_k,u_k,\tilde{A}_k)+(F_{1,k}+M_{1,k}\Gamma_{1,k}N_{1,k})\tilde{x}_k \\ \quad +O(\tilde{x}_k{}^2)+w_k \\ y_{k+1}=h(\hat{x}_{k+1},\tilde{B}_{k+1})+(H_{2,k+1}+M_{2,k+1}\Gamma_{2,k+1}N_{2,k+1})\tilde{x}_{k+1} \\ +O(\tilde{x}_{k+1}{}^2)+v_{k+1} \end{cases} \tag{21}$$

C. Error Covariance Matrix

Prediction error $\tilde{x}^-_{k+1}$, state estimation error $\tilde{x}^+_{k+1}$, output prediction error $\tilde{y}_{k+1}$, one-step state prediction error covariance P^-_{k+1}, output prediction error covariance $P_{y,k+1}$ and state estimation error covariance P^+_{k+1} are defined as:

$$\begin{cases} \tilde{x}^-_{k+1}=x_{k+1}-\hat{x}^-_{k+1} \\ \tilde{y}_{k+1}=y_{k+1}-\hat{y}_{k+1} \\ \tilde{x}^+_{k+1}=x_{k+1}-\tilde{x}^+_{k+1} \end{cases},\begin{cases} P^-_{k+1}=E(\tilde{x}^-_{k+1}\tilde{x}^-_{k+1}{}^{\mathrm{T}}) \\ P_{y,k+1}=E(\tilde{y}_{k+1}\tilde{y}_{k+1}{}^{\mathrm{T}}) \\ P^+_{k+1}=E(\tilde{x}^+_{k+1}\tilde{x}^+_{k+1}{}^{\mathrm{T}}) \end{cases} \tag{22}$$

The one-step prediction estimation of the model state obtained by the cubature Kalman filter algorithm is as follows:

$$\hat{x}^-_{k+1}=f(\hat{x}^+_k,u_k,\tilde{A}_k)+O(\tilde{x}_k^{+2}) \tag{23}$$

The linear expression of state variables in equation (21) and equation (23) are introduced into the prediction error expression, and the expansion term above the third order is ignored.

$$\tilde{x}^-_{k+1}=(F_{1,k}+M_{1,k}\Gamma_{1,k}N_{1,k})\tilde{x}^+_k+w_k \tag{24}$$

Furthermore, the covariance of state prediction error was obtained

$$\begin{aligned} P^-_{k+1}&=(F_{1,k}+M_{1,k}\Gamma_{1,k}N_{1,k})P^+_k(F_{1,k}+M_{1,k}\Gamma_{1,k}N_{1,k})^{\mathrm{T}} \\ &+Q_k \end{aligned} \tag{25}$$

In the same way, the estimated values of system observation were as follows:

$$\hat{y}_{k+1}=h(\hat{x}^-_{k+1},\tilde{B}_{k+1})+O(\tilde{x}^-_{k+1}{}^2) \tag{26}$$

By introducing equation (21) and equation (26) into equation (22), it is obtained that:

$$\tilde{y}_{k+1}=(H_{2,k+1}+M_{2,k+1}\Gamma_{2,k+1}N_{2,k+1})\tilde{x}^-_{k+1}+v_{k+1} \tag{27}$$

The output prediction error covariance is obtained:

$$\begin{aligned} P_{y,k+1}&=(H_{2,k+1}+M_{2,k+1}\Gamma_{2,k+1}N_{2,k+1})\bullet P^-_{k+1} \\ &\bullet(H_{2,k+1}+M_{2,k+1}\Gamma_{2,k+1}N_{2,k+1})^{\mathrm{T}}+R_{k+1} \end{aligned} \tag{28}$$

D. Robust cubature Kalman filter design

Lemma 1[17]: There are matrices A, B, C and D with appropriate dimensions, satisfying $CC^{\mathrm{T}}\le I$. If a real positive definite matrix and a normal number κ are given, and $\kappa I-DUD^T>0$ is satisfied, the following inequality holds true:

$$\frac{(A+BCD)U(A+BCD)^{\mathrm{T}}}{A(U^{-1}-\kappa^{-1}D^{\mathrm{T}}D)^{-1}A^{\mathrm{T}}+\kappa BB^{\mathrm{T}}}\le 1 \tag{29}$$

Lemma 2[18]: Suppose there is a real symmetric matrix $U=U^{\mathrm{T}}>0$. There are functions $e_k(U)=e_k^{\mathrm{T}}(U^{\mathrm{T}})\in\mathrm{R}^{l\times l}$ and $g_k(U)=g_k^{\mathrm{T}}(U^{\mathrm{T}})\in\mathrm{R}^{l\times l}$, where $0\le k\le l$. If there is a real symmetric matrix $V=V^{\mathrm{T}}>U$, the following conditions are satisfied:

$$\begin{aligned} e_k(V)&\ge e_k(U) \\ g_k(V)&\ge g_k(U) \end{aligned} \tag{30}$$

Then there are solutions X_k and Y_k of the following equation satisfying $X_k\le Y_k$:

$$X_k=e_k(X_{k-1}),Y_k=g_k(Y_{k-1}),X_0=Y_0 \tag{31}$$

According to lemma 1 and formulas (25) and (28), the upper bounds Σ^-_{k+1} and $\Sigma_{y,k+1}$ of prediction error covariance with uncertain parameters and output prediction error covariance were obtained:

$$\begin{aligned} P^-_{k+1}&\le F_{1,k}((\Sigma^+_k)^{-1}-\kappa_1{}^{-1}N^{\mathrm{T}}_{1,k}N_{1,k})^{-1}F^{\mathrm{T}}_{1,k} \\ &+\kappa_1M_{1,k}M^{\mathrm{T}}_{1,k}+Q_k=\Sigma^-_{k+1} \end{aligned} \tag{32}$$

$$\boldsymbol{P}_{y,k+1} \le \boldsymbol{H}_{2,k+1}((\boldsymbol{\Sigma}_{k+1}^-)^{-1} - \kappa_2^{-1}\boldsymbol{N}_{2,k+1}^{\mathrm{T}}\boldsymbol{N}_{2,k+1})^{-1}\boldsymbol{H}_{2,k+1}^{\mathrm{T}} + \kappa_2\boldsymbol{M}_{2,k+1}\boldsymbol{M}_{2,k+1}^{\mathrm{T}} + \boldsymbol{R}_{k+1} = \boldsymbol{\Sigma}_{y,k+1} \tag{33}$$

According to the conclusion of lemma 2, formula (25) is taken as the function e, and formula (28) as the function g. It is easy to prove that if the one-step prediction covariance satisfies $\boldsymbol{P}_{k+1}^- \le \boldsymbol{\Sigma}_{k+1}^-$, the state error covariance satisfies $\boldsymbol{P}_{k+1}^+ \le \boldsymbol{\Sigma}_{k+1}^+$. Therefore, the trace of the upper bound of the error covariance matrix can be minimized by selecting the appropriate gain matrix. Namely if $\boldsymbol{P}$ is replaced by $\boldsymbol{\Sigma}$, the minimum upper bound of error covariance for state estimation of systems with parameter uncertainty can be obtained.

It can be seen from formulas (17) and (20) that $\boldsymbol{F}_{1,k}$ and $\boldsymbol{H}_{2,k+1}$ are the first-order error coefficients of the state equation and the measurement equation respectively. Therefore, in order to improve the accuracy of error covariance estimation, cubature transform can be used to calculate the error covariance matrix of uncertain parameter system, instead of $\boldsymbol{F}_{1,k}(\boldsymbol{\Sigma}_k^+ - \kappa_1^{-1}\boldsymbol{N}_{1,k}^{\mathrm{T}}\boldsymbol{N}_{1,k})^{-1}\boldsymbol{F}_{1,k}$ and $\boldsymbol{H}_{2,k+1}(\boldsymbol{\Sigma}_{k+1|k} - \kappa_2^{-1}\boldsymbol{N}_{2,k+1}^{\mathrm{T}}\boldsymbol{N}_{2,k+1})^{-1}\boldsymbol{H}_{2,k+1}$ terms in the upper bound of covariance. When calculating the cubature point, the upper bound of the covariance of the prior distribution of the state variables is replaced by formulas (34) and (35) respectively.

$$\hat{\boldsymbol{\Sigma}}_k^+ = ((\boldsymbol{\Sigma}_k^+)^{-1} - \kappa_1^{-1}\boldsymbol{N}_{1k}^{\mathrm{T}}\boldsymbol{N}_{1k})^{-1} \tag{34}$$

$$\hat{\boldsymbol{\Sigma}}_{k+1}^- = ((\boldsymbol{\Sigma}_{k+1}^-)^{-1} - \kappa_2^{-1}\boldsymbol{N}_{2,k+1}^{\mathrm{T}}\boldsymbol{N}_{2,k+1})^{-1} \tag{35}$$

Finally, the upper bound of the error covariance is obtained by calculating the cubature point with the spherical radial criterion, as shown in formula (36) (37) (38).

$$\boldsymbol{\Sigma}_{k+1}^- = \frac{1}{2n}\sum_{i=1}^{2n}(\boldsymbol{X}_{i,k+1}^- - \hat{\boldsymbol{x}}_{k+1}^-)(\boldsymbol{X}_{i,k+1}^- - \hat{\boldsymbol{x}}_{k+1}^-)^{\mathrm{T}} + \kappa_1\boldsymbol{M}_{1,k}\boldsymbol{M}_{1,k}^{\mathrm{T}} + \boldsymbol{Q}_k \tag{36}$$

$$\boldsymbol{\Sigma}_{y,k+1} = \frac{1}{2n}\sum_{i=1}^{2n}(\boldsymbol{Y}_{i,k+1} - \hat{\boldsymbol{y}}_{k+1})(\boldsymbol{Y}_{i,k+1} - \hat{\boldsymbol{y}}_{k+1})^{\mathrm{T}} + \kappa_2\boldsymbol{M}_{2,k+1}\boldsymbol{M}_{2,k+1}^{\mathrm{T}} + \boldsymbol{R}_{k+1} \tag{37}$$

$$\boldsymbol{\Sigma}_{xy,k+1} = \frac{1}{2n}\sum_{i=1}^{2n}(\boldsymbol{X}_{i,k+1}^- - \hat{\boldsymbol{x}}_{k+1}^-)(\boldsymbol{Y}_{i,k+1} - \hat{\boldsymbol{y}}_{k+1})^{\mathrm{T}} \tag{38}$$

In lemma 1, the upper bound of the state error covariance matrix of the system with parameter uncertainty is expressed by the covariance matrix with parameter uncertainty κ.

In robust cubature Kalman filter algorithm, the lower limit of κ is restricted by condition $\hat{\boldsymbol{\Sigma}}_{k|k} = (\boldsymbol{\Sigma}_{k|k}^{-1} - \kappa_1^{-1}\boldsymbol{N}_{1k}^{\mathrm{T}}\boldsymbol{N}_{1k})^{-1}$ and $\hat{\boldsymbol{\Sigma}}_{k+1|k} = (\boldsymbol{\Sigma}_{k+1|k}^{-1} - \kappa_2^{-1}\boldsymbol{N}_{2k}^{\mathrm{T}}\boldsymbol{N}_{2k})^{-1}$, and κ must be greater than the maximum eigenvalue of matrix $\boldsymbol{N}^{-1}\boldsymbol{\Sigma}(\boldsymbol{N}^{\mathrm{T}})^{-1}$. In general, the matrix $\boldsymbol{N}$ is the identity matrix. Therefore:

$$\kappa > \max(\mathrm{eig}(\boldsymbol{\Sigma})) \tag{39}$$

(a) When $\kappa \gg \max(\mathrm{eig}(\boldsymbol{\Sigma}))$, the conditions in the algorithm are satisfied. In that case, $(\boldsymbol{\Sigma}^{-1} - \kappa^{-1}\boldsymbol{N}^{\mathrm{T}}\boldsymbol{N})^{-1}$ is approximately unchanged, but $\kappa\boldsymbol{M}\boldsymbol{M}^{\mathrm{T}}$ tends to be infinite. The system error covariance matrix has no limitation on the uncertainty of the system, so the algorithm fails.

(b) When $\kappa = \max(\mathrm{eig}(\boldsymbol{\Sigma})) + \delta$, where δ is an arbitrary small quantity, $\max((\mathrm{eig}(\boldsymbol{\Sigma}^{-1} - \kappa^{-1}\boldsymbol{N}^{\mathrm{T}}\boldsymbol{N})^{-1}))$ is much larger than $\max(\mathrm{eig}(\boldsymbol{\Sigma}^{-1})^{-1})$. With the increase of iteration steps, the error covariance matrix tends to diverge, and the divergence rate increases with the decrease of δ value.

(c) When the covariance matrix of N state variables in the system has a large order of magnitude difference, κ needs to satisfy the condition $\kappa > \max(\mathrm{eig}(\boldsymbol{\Sigma}))$. According to inequality (32), the larger κ is, the larger upper bound for the covariance of the state variables with smaller order of magnitude it defines, which makes the algorithm more conservative for the estimated values of the state variables with smaller covariance, resulting in some elements of higher accuracy than others in the filtering results.

VI. Uncertainty Setting of Filter Estimation

A. *Uncertainty of projectile motion parameters*

In general, the impact point of guided ammunition obeys normal distribution $N(\mu, \sigma^2)$. In the case of confidence level $(1-\alpha)$, the confidence interval of variance σ^2 is as follows:

$$\left(\frac{(n-1)S^2}{\chi_{\frac{\alpha}{2}}^2(n-1)}, \frac{(n-1)S^2}{\chi_{1-\frac{\alpha}{2}}^2(n-1)}\right) \tag{40}$$

Take the confidence interval as $(0.9\hat{\sigma}, 1.15\hat{\sigma})$. Check the distribution table χ^2, when $N = 1000$, the confidence level is greater than 99%.

The six degree of freedom motion model of missile body in Fig. 4 was constructed by MATLAB. The initial velocity of the projectile was set at 270m/s, the firing angle was 78.91°, the standard meteorological conditions of artillery were adopted, and the target point was set as $(2000, 0, 0)$ in the ground coordinate system. The standard deviation of all actual ballistic parameters relative to ideal ballistic parameters was calculated as the uncertainty of system parameters. Finally, the standard deviation curve of each parameter is shown in Fig. 5.

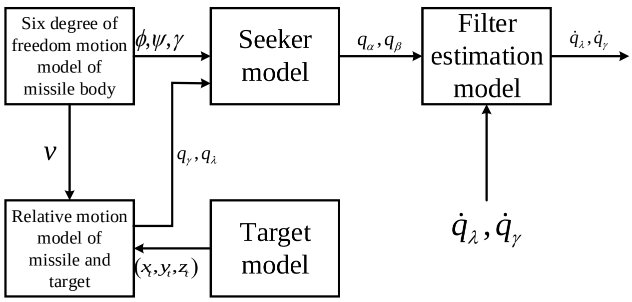

Fig. 4. Simulation verification model

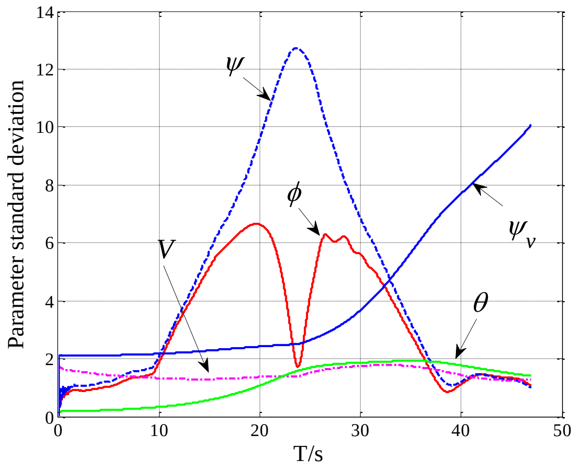

(a) Standard deviation curve of error of partial angle parameter

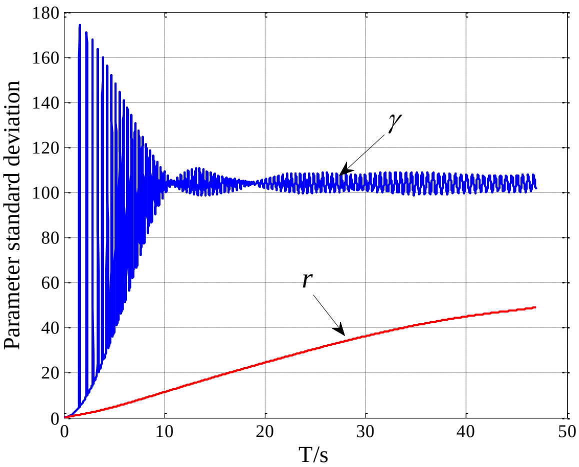

(b) Standard deviation curve of error of roll angle and distance parameters

Fig. 5. Error standard deviation curve of projectile motion parameters

In Fig. 5, at the end of the trajectory, the standard deviation of pitch angle ϕ, yaw angle ψ, velocity v and inclination angle θ of the missile body is small, and so is the influence of uncertainty. The measurement error of distance r for guided mortar projectile is very small compared with the distance between missile and target, and the distance measurement can be conducted by low-cost components, so the influence of uncertainty is small. The standard deviation of roll angle γ and ballistic deflection angle ψ_V is large, which has great influence on filtering.

B. Robust design of LOS angular rate estimation

According to equations (9) and (11), the Jacobian matrix of the state equation of the filtering model and the measurement equation for the state variables can be obtained, namely the first-order coefficient matrix:

$$\boldsymbol{F}=\begin{bmatrix}\frac{\partial \dot{q}_\lambda}{\partial q_\lambda} & \frac{\partial \dot{q}_\lambda}{\partial q_\gamma}\\ \frac{\partial \dot{q}_\gamma}{\partial q_\lambda} & \frac{\partial \dot{q}_\gamma}{\partial q_\gamma}\end{bmatrix},\boldsymbol{H}=\begin{bmatrix}\frac{\partial q_\alpha}{\partial q_\lambda} & \frac{\partial q_\alpha}{\partial q_\gamma}\\ \frac{\partial q_\beta}{\partial q_\lambda} & \frac{\partial q_\beta}{\partial q_\gamma}\end{bmatrix} \tag{41}$$

Then, the Jacobian matrix of the first-order coefficient matrix for the uncertain parameters (i.e. projectile motion parameters) can be obtained:

$$\boldsymbol{J}_F=\begin{bmatrix}\frac{\partial f_{11}}{\partial \xi} & \frac{\partial f_{12}}{\partial \xi}\\ \frac{\partial f_{21}}{\partial \xi} & \frac{\partial f_{22}}{\partial \xi}\end{bmatrix},\boldsymbol{J}_H=\begin{bmatrix}\frac{\partial h_{11}}{\partial \boldsymbol{\eta}} & \frac{\partial h_{12}}{\partial \boldsymbol{\eta}}\\ \frac{\partial h_{21}}{\partial \boldsymbol{\eta}} & \frac{\partial h_{22}}{\partial \boldsymbol{\eta}}\end{bmatrix} \tag{42}$$

Where $f_{11}\sim f_{22}$ are elements in the coefficient matrix $\boldsymbol{F}$ of the linearized equation of state. $h_{11}\sim h_{22}$ are elements in the coefficient matrix $\boldsymbol{H}$ of the linearized measurement equation. $\xi=[v \quad \theta \quad \psi_v]$ is the uncertain parameter of the equation of state. $\boldsymbol{\eta}=[\phi \quad \psi]$ is the uncertain parameter of the measurement equation.

According to formulas (17)(20), the uncertainty of filtering system can be obtained:

$$\begin{cases}\boldsymbol{M}_1\boldsymbol{\Gamma}_1\boldsymbol{N}_1=\boldsymbol{J}_U\times \mathrm{diag}(\max(\mathrm{abs}(\Delta\xi)) \quad \max(\mathrm{abs}(\Delta\xi)))^{\mathrm{T}}\\ \boldsymbol{M}_2\boldsymbol{\Gamma}_2\boldsymbol{N}_2=\boldsymbol{J}_V\times \mathrm{diag}(\max(\mathrm{abs}(\Delta\boldsymbol{\eta})) \quad \max(\mathrm{abs}(\Delta\boldsymbol{\eta})))^{\mathrm{T}}\end{cases}$$

(43)

Where $\Delta\xi$ and $\Delta\boldsymbol{\eta}$ are the deviation values between the actual ballistic parameters and the ideal ballistic parameters. The operator "diag" represents a diagonal matrix. When designing the filter, $\max(\mathrm{abs}(\Delta\xi))$ and $\max(\mathrm{abs}(\Delta\boldsymbol{\eta}))$ take the standard deviation of the error between the actual trajectory and the ideal trajectory calculated by Monte Carlo simulation method at the corresponding time.

VII. Simulation Verification and Analysis

In order to verify the performance of the algorithm, the filtering algorithm is simulated as shown in Fig 4. The detection range of seeker is 3000m, and the filtering estimation models are CKF and RCKF designed in this paper. Set $\kappa=19.2\max(\mathrm{eig}(\boldsymbol{\Sigma}))$.

The interference of ballistic parameters includes projectile mass, moment of inertia, aerodynamic parameters, angle deviation, initial velocity deviation, wind and so on. Due to the small error of mass and moment of inertia, its influence is ignored. The list of interference items is shown in Table II. The CKF algorithm and the designed RCKF algorithm were used to filter and estimate the LOS angle and angular rate of the missile and target under the interference condition.

Table II
The List of Interference Items

Interference term	Decimal value (3σ)	Large value (3σ)
Deviation of axial force coefficient /%	1.2	4
Deviation of normal force coefficient /%	0.8	2
Deviation of lateral force coefficient /%	0.8	2
Deviation of pitching moment coefficient /%	1	5
Deviation of yaw moment coefficient /%	1	5
Deviation of rolling moment coefficient /%	1	5
Angle deviation/°	0.1	1.0
Initial velocity deviation/(m/s)	0.2	5.0
wind speed/(m/s)	0.3	1.0
wind direction/°	0	90

As shown in Fig. 6, Fig. 7, Fig. 8 and Fig. 9, the difference between the estimation results of the CKF and the RCKF designed in this paper is not particularly large, and they can basically be estimated around the the true value of line of sight angle or angular rate.

The maximum deviation and standard deviation of line of sight angle and angular rate estimated by filtering under the condition of large and small interference were calculated and listed in Table III and Table IV. It can be concluded from Fig. 6, Fig. 7 and Table III that the filtering accuracy of RCKF is slightly better than that of CKF, and the results of CKF are also in the acceptable range, which also proves the effectiveness of RCKF algorithm. Although the accuracy of angle and angular rate are improved to a certain extent, there is little difference between them. The main reason is that under the condition of small disturbance, the disturbance is small, the change of ballistic motion parameters is small, the system uncertainty is small, and the impact on CKF is small.

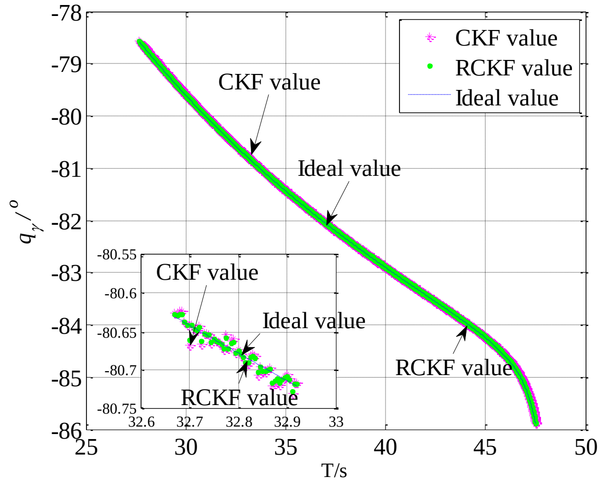

(a) Estimation of inclination angle of LOS

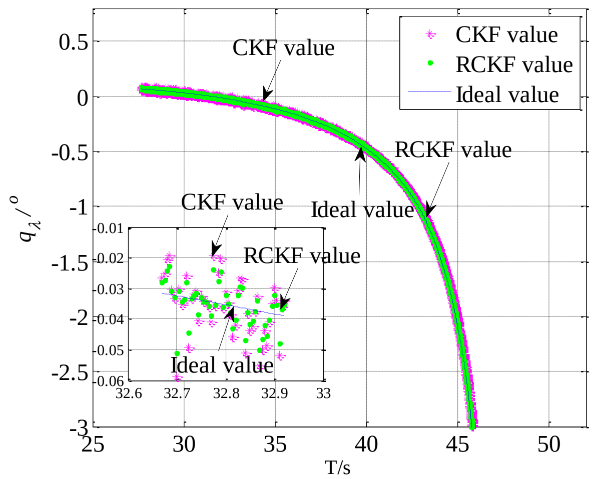

(b) Estimation of deviation angle of LOS

Fig. 6. Estimation of LOS angle under small interference

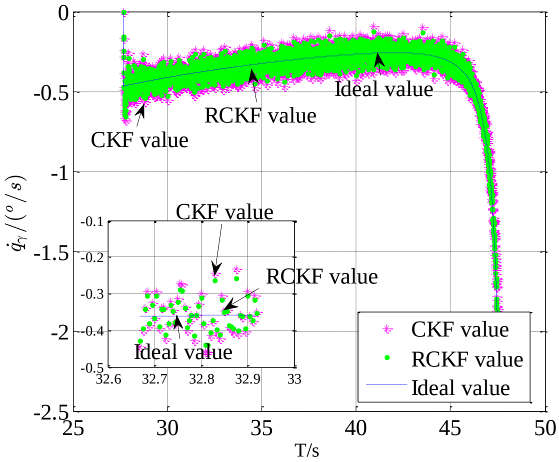

(a) Inclination angular rate of LOS

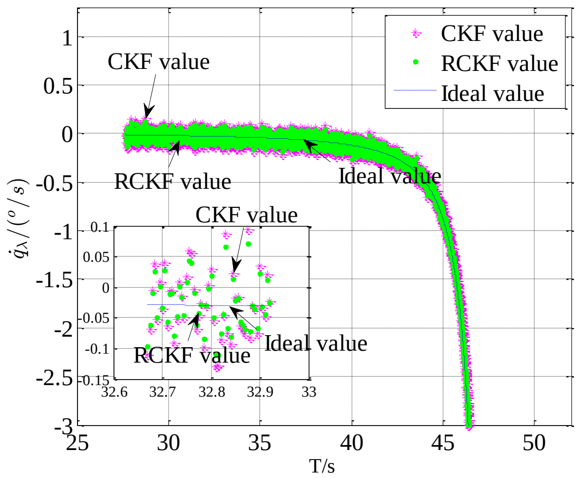

(b) Deviation angular rate of LOS

Fig. 7. Estimation of LOS angular rate under small interference

TABLE III
ERROR AND STANDARD DEVIATION UNDER SMALL DISTURBANCE

Parameter	Maximum error of CKF / (º)	Maximum error of RCKF / (º)	Standard deviation of CKF / (º)	Standard deviation of RCKF / (º)
q_γ	0.034	0.024	0.0091	0.0065
q_λ	0.036	0.022	0.0087	0.0061
$\dot{q}_\gamma$	0.298	0.297	0.0507	0.0419
$\dot{q}_\lambda$	0.275	0.262	0.0513	0.0426

It can be concluded from Fig. 8, Fig. 9 and Table IV that under the condition of large disturbance, the filtering accuracy of RCKF is significantly higher than that of CKF, and the error of CKF result is large, which is unacceptable. RCKF shows obvious robustness when the uncertainty of missile parameters is large. For the estimation of line of sight inclination angle, the maximum error is reduced by 55.56%, and the standard deviation is reduced by 55.53%. For the estimation of line of sight deflection angle, the maximum error is reduced by 56.5%, and the standard deviation is reduced by 55.51%. For the estimation of line of sight inclination angular rate, the maximum error decreases by 53.92%, and the standard deviation decreases by 55.96%. For the estimation of line of sight deflection angular rate, the maximum error decreases by 55.57%, and the standard deviation decreases by 55.41%.

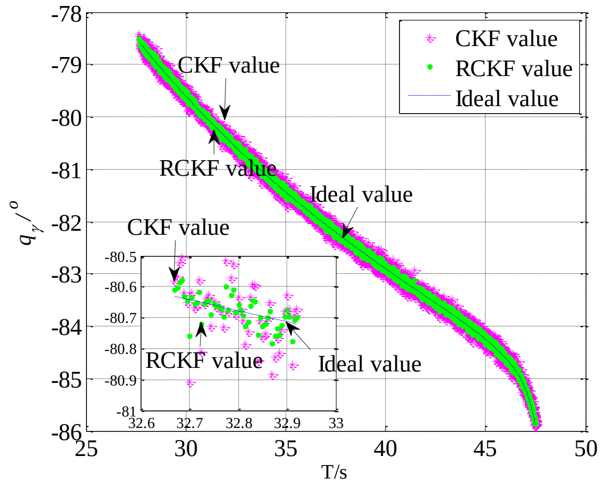

(a) Estimation of inclination angle of LOS

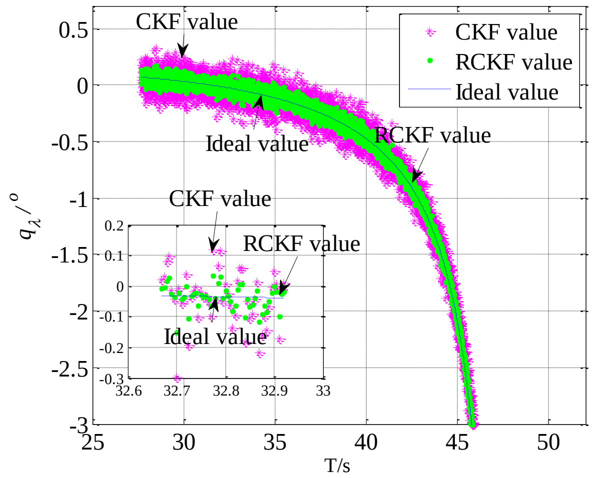

(b) Estimation of deviation angle of LOS

Fig. 8. Estimation of LOS angle under big interference

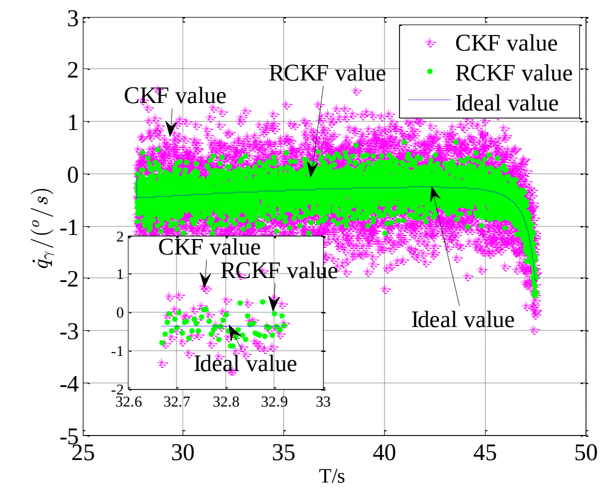

(a) Inclination angular rate of LOS

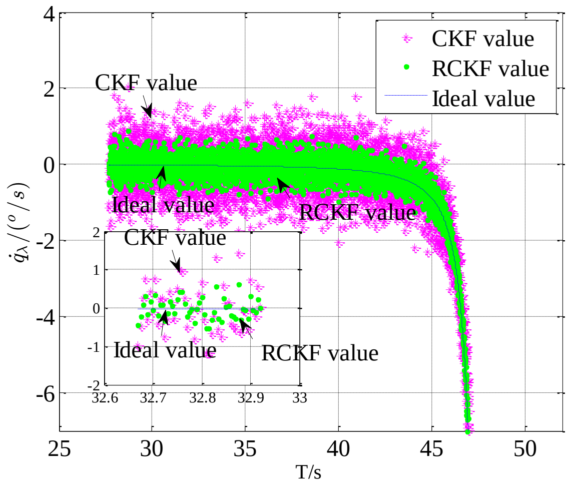

(b) Deviation angular rate of LOS

Fig. 9. Estimation of LOS angular rate under big interference

TABLE IV
ERROR AND STANDARD DEVIATION UNDER BIG DISTURBANCE

Parameter	Maximum error of CKF / (°)	Maximum error of RCKF / (°)	Standard deviation of CKF / (°)	Standard deviation of RCKF / (°)
q_γ	0.3407	0.1514	0.0918	0.0408
q_λ	0.3208	0.1394	0.0895	0.0398
$\dot{q}_\gamma$	2.2026	1.0137	0.6011	0.2651
$\dot{q}_\lambda$	2.0525	0.9122	0.5719	0.2544

To sum up, by comparing the filtering results of large and small disturbances, it can be concluded that the RCKF algorithm has robustness in the case of large model parameter uncertainty and improves the filtering accuracy of the algorithm.

VIII. CONCLUSION

In order to reduce the cost of guided ammunition, the missile target motion model and seeker model were used to estimate the LOS angle and angular rate, and trajectory parameters were used to replace the IMU. Based on the uncertainty of filtering model parameters, a RCKF filtering method for uncertain parameter model was proposed. The problem of filter estimation for uncertain parameter model was transformed into the problem of minimum upper bound of error covariance matrix with parameter κ to overcome the influence of parameter uncertainty on filter estimation accuracy. The effectiveness and robustness of the algorithm were proved by digital simulation, which provided a reference for the low cost of guided ammunition.

REFERENCES

[1] Tingting Sun, Hairong Chu, Hongguang Jia, et al. “Line-of-sight angular rate decoupling and estimation of strapdown optical seeker,” *Infrared and Laser Engineering,* vol. 43, no. 5, pp. 1587-1593, May. 2014.

[2] Bin Zhao, Jun Zhou. “Attitude Dynamics Aiding for Line-of-Sight Angular Rate Reconstruction of Strap-down Seeker,” *Proceedings of the 34th Chinese Control Conference,* Hangzhou, China, 2015, pp. 5079-5083.

[3] Changzhu Wei, Yepeng Han, Naigang Cui. “Fifth-Degree Cubature Kalman Filter Estimation of Seeker Line-of-Sight Rate Using Augmented-Dimensional Model,” *JOURNAL OF GUIDANCE, CONTROL, AND DYNAMICS,* May. 2017, doi: 10.2514/1.G002809.

[4] M. J. Maley. “Line of Sight Rate Estimation for Guided Projectiles with Strapdown Seekers,” *AIAA Guidance, Navigation, and Control*

Conference, Kissimmee, Florida, USA, 2015, pp. 1-24.

[5] K. D. Solomon Raj, I. S. Satya Ganesh. "Estimation of Line-of-Sight Rate in a Homing Missile Guidance Loop using Optimal Filters," *IEEE ICCSP 2015 conference*, 2015, pp. 0398-0402.

[6] Shaoming He, Wei Wang and Jiang Wang. "Robust finite-time line-of-sight angular rate estimation in missile guidance," *Journal of Aerospace Engineering,* pp. 1-10, June. 2016, doi: 10.1 177/0954410016654178.

[7] Pei Wang, Ke Zhang, Cong Nie. "Research on Line-of-Sight Rate Estimation of Strapdown Seeker," *Applied Mechanics and Materials,* pp. 3739-3744, May, 2014, doi:10.4028/www.scientific. net/AMM.556-562.3739.

[8] Zhijun Yu, Jianming Wei, Haitao Liu. "A new adaptive maneuvering target tracking algorithm using artificial neural networks," *Proc. of the international Joint Conferemce on neural networks,* 2008, pp. 901-905.

[9] Guobin Chang. "Kalman filter with both adaptivity and robustness," *Journal of Process Control,* vol. 24, pp. 81-87, 2014, doi: 10.1016/j.jprocont.2013.12.017.

[10] R. Panigrahi, B. Subudhi. "Performance Enhancement of Shunt Active Power filter using a Kalman Filter based $H\infty$ Control Strategy," *IEEE Transactions on Power Electronics,* pp. 1-1, 2016, doi: 10.1109/TPEL.2016.2572142.

[11] Yang Meng, Shesheng Gao, Yongmin Zhong, et al. "Covariance matching based adaptive unscented Kalman filter for direct filtering in INS/GNSS integration," *Acta Astronautica,* vol. 120, pp. 171-181, 2016, doi: 10.1016/j.actaastro.2015.12.014.

[12] Yunlong Shang, Chenghui Zhang, Naxin Cui, et al. "State of charge estimation for lithium-ion batteries based on extended Kalman filter optimized by fuzzy neural network," *Control Theory & Applications,* vol. 33, no. 2, pp. 213-220, 2016, doi: 10.7641/CTA.2016.41167.

[13] S. A. Nahian, P. L. Nguyen, H. G. Park, et al. "Real-time sensor fault tolerant control for an Electro-hydraulic actuator," *KSFC 2015 Autumn Conference on Drive &Control,* 2015, pp. 167-172.

[14] Wei Zhao. "RESEARCH AND APPLICATIONS OF ROBUST KALMAN FILTERING ALGORITHM BASED ON CUBATURE-RULE," *Ph.D. dissertation, Dept. Con. Eng., Yanshan Univ*., Qin Huangdao, Hebei, China, 2017.

[15] Xingfang Qian, "Missile Flight Mechanics," Beijing, China, *BEIJING INSTITUTE OF TECHINOLOGY PRESS*, 2016, pp. 2-49.

[16] Zipeng Han, "Exterior ballistics," Beijing, China, *BEIJING INSTITUTE OF TECHINOLOGY PRESS*, 2008, pp. 23-150.

[17] Min Gao, Yongwei Zhang and Suochang Yang. "Firing Control Optimization of Impulse Thrusters for Trajectory Correction Projectiles," *International Journal of Aerospace Engineering,* Volume 2015, Article ID 781472, 11 pages, Apr, 2015, 10.1155/2015/781472.

[18] L. H. Xie, C. Y. Soh, D. Souza. "Robust Kalman Filtering for Uncertain Discrete-Time Systems," *IEEE TRANSACTIONS ON AUTOMATIC CONTROL,* vol. 39, no. 6, pp. 1310-1314, 1994, doi: 10.1109/9.293203.